IL NUOVO CIMENTO Vol. 117 B, N. 9-11 Settembre-Novembre 2002

The latest view of the Early Universe(*)

P. de Bernardis and S. Masi
Università di Roma "La Sapienza" - Rome, Italy

(ricevuto il 4 Novembre 2002; approvato il 4 Dicembre 2002)

Summary. — The Big Bang Nucleosynthesis (so beautifully pioneered by Enrico Fermi) and the Cosmic Microwave Background (CMB) are closely linked and offer complementary tools to investigate the Early Universe. We shortly review this topic and focus on the latest results on the CMB. Resolved images of the CMB produced by the BOOMERanG, MAXIMA and DASI experiments allow a detailed study of the physical processes taking place before recombination, depicting a consistent new cosmology. We present the experimental evidence, the current interpretation of the data, the problems still open, and the future activity in this field.

PACS 98.70.Vc – Background radiations.
PACS 01.30.Cc – Conference proceedings.

1. – Observables of the Early Universe

Our expanding Universe was denser and hotter in the past. It has evolved from a primeval fireball, a very hot and dense state where matter and radiation were in thermal equilibrium. Light elements were produced in the primeval fireball, and the primordial abundances of these elements are measurable now in selected regions of the local Universe, where they are still unprocessed. The synthesis of light nuclei happened in the presence of a huge number of photons ($\sim 10^9$ for each baryon). These photons are now visible as a faint glow of microwaves, the Cosmic Microwave Background (CMB).

The photons of the CMB play a key role in the formation of light elements. They photo-dissociate nuclei impeding their formation until the temperature decreases below $\sim 10^9$ K. Their energy density dominates the expansion and the temperature behaviour of the primeval fireball. Temperature and expansion rate affect very significantly the ratio n/p and the synthesis rates.

(*) Paper presented at the IX ICRA Network Workshop "Fermi and Astrophysics" (Rome, Pescara, September 2001) held under the auspices of the Italian Committee for the Celebration of the Hundredth Anniversary of the birth of Enrico Fermi. Joint copyright SIF and World Scientific.

The Hot Big Bang theory is able to predict from first principles the observable quantities described above, thus allowing observational tests of the physics of the Early Universe. Together with the observed recession of galaxies, the abundances of light elements and the thermal spectrum of the CMB are the three pillars of modern cosmology. Recent reviews on these aspects can be found in [1] and [2].

It is very remarkable that all these observations are fit simultaneously by the simple scenario of Hot Big Bang cosmology. However, while the big picture is very robust, there are still unexplained issues, which are currently investigated using high sensitivity measurements of the same observables. Here we focus on one of these cosmology tools, the image of the CMB, which has been recently resolved by CMB anisotropy experiments.

2. – CMB anisotropy

The CMB is an isotropic 2.73 K black body and contains most of the photons present in our universe. These thermal photons interacted with matter (via Thomson scattering) only as long as the Universe has been in a ionized state (the initial homogeneous "primeval fireball" [3]). After that, they traveled freely for about 15 billion years before reaching our microwave telescopes. The map of the CMB is thus a map of an early phase of our Universe.

We believe that gravitational instability has grown the large scale structure of the present Universe from small density fluctuations seeds, which were present in the primeval fireball, and are now evident in high resolution images of the CMB. The two observables are thus tightly linked, sampling respectively an early state and the final result of the process of formation of structures. Moreover, the inflation hypothesis links these seeds to quantum fluctuations in a scalar field present in the very early Universe, immediately after the Big Bang (see, *e.g.*, [4]): the CMB is thus a window on the first split second of the evolution of the Universe, when the energy was much higher than the ones we can investigate in the laboratory.

When we look to the CMB, we detect photons scattered from the edge of the primeval plasma (last scattering surface, LSS), which has been present in the Universe for $t \lesssim 300000$ y. This is the time required to cool down the primeval fireball below 3000 K, where ionized hydrogen can become neutral: such a process is called recombination. The causal horizon at that epoch is seen under an angle of $\sim 1^\circ$, the exact value depending mainly on the curvature of the Universe, but also on its detailed composition, and, at a smaller extent, on the expansion rate H_o. The subtended angle can be estimated naively by noting that on the LSS the size of the causal horizon is of the order of 300000 light years; we look from a distance of about 15 billion light years (basically corresponding to the age of the universe) and after an expansion of the Universe by a factor ~ 1000. The subtended angle, in a Euclidean universe, will then be $\theta \sim 10^3 \times 3 \times 10^5 / 15 \times 10^9$ rad $\sim 1^\circ$.

Density perturbations $\Delta\rho/\rho$ in the primeval plasma of photons and matter with dimensions smaller than the horizon undergo acoustic oscillations. These are the result of the opposite effects of self-gravity and of the pressure of the photons. In fact, the ratio between the number density of CMB photons and the number density of matter particles is $\sim 10^9$, so photon pressure plays an important role in the dynamics of the primeval plasma. Structures larger than the horizon, instead, are basically frozen, since there is not enough time for forces to propagate from one edge of the perturbation to the opposite one.

There are three physical processes converting the density perturbations present at recombination into *observable* CMB temperature fluctuations $\Delta T/T$. They are: the

photon density fluctuations δ_γ, which can be related to the matter density fluctuations $\Delta\rho$ once a specific class of perturbations, *e.g.*, adiabatic, is specified; the gravitational redshift of photons scattered in an over-density or an under-density with gravitational potential difference ϕ_r; the Doppler effect produced by the proper motion with velocity v of the electrons scattering the CMB photons. In formulas:

$$\frac{\Delta T}{T}(\vec{n}) \approx \frac{1}{4}\delta_{\gamma r} + \frac{1}{3}\frac{\phi_r}{c^2} - \vec{n}\frac{\vec{v_r}}{c}\,, \tag{1}$$

where $\vec{n}$ is the line-of-sight vector and the subscript r labels quantities at recombination.

We thus expect to see the characteristic scale of the acoustic horizon imprinted in the image of the CMB. This means that if we compute the angular power spectrum of the image, we expect to see a peak at an angular scale $\theta \sim 1^o$. If, as general relativity allows, the curvature of the Universe at large scales is not vanishing, the photons will travel along curved paths between the LSS and us, and the horizon can be either magnified (positive curvature, high density of the Universe, larger spots) or de-magnified (negative curvature, low density of the Universe, smaller spots). The measurement of this angular scale can thus be used to measure the curvature of the universe (see, *e.g.*, [5]).

To see how this works, we can compute the angular diameter θ subtended by the acoustic horizon as $\theta \sim d/D_A$, where d is the proper length of the acoustic horizon at recombination and D_A is the angular diameter distance of recombination. Using the Friedmann equation for the scale factor of the Universe a, we can compute d as (see, *e.g.*, [6])

$$d = \int_0^{t_{\rm rec}} c_s \mathrm{d}t = \int_0^{a_{\rm rec}} c_s \frac{\mathrm{d}a}{\dot{a}} = \int_0^{1/(1+z_{\rm rec})} \frac{c_s(\hat{a})\mathrm{d}\hat{a}}{H_o\hat{a}\sqrt{\Omega_{\gamma o}\hat{a}^{-4} + \Omega_{Mo}\hat{a}^{-3} + \Omega_\Lambda + (1-\Omega)\hat{a}^{-2}}}\,, \tag{2}$$

where $\hat{a} = a/a_o$, a_o is the present value of the scale factor; $z = a_o/a - 1$ is the redshift, and c_s is the sound speed in the primeval plasma

$$c_s = \frac{c}{\sqrt{3(1 + \frac{3\Omega_{bo}}{4\Omega_{\gamma o}}a)}}\,. \tag{3}$$

H_o is the present expansion rate of the Universe (Hubble constant ~ 70 km/s/Mpc), the Ω_{io}, $i = \gamma, M, \Lambda$ are the energy densities of photons, matter and dark energy, respectively, all normalized to the critical density $\rho_c = 3H_o^2/8\pi G$, and $\Omega = \Omega_{\gamma o} + \Omega_{Mo} + \Omega_\Lambda$.

For $\Omega \sim 1$, before recombination there is a relatively long period when the Universe is dominated by matter: radiation and dark energy are negligible between equivalence and recombination. In such a case, the integral above can be approximated as

$$d \sim \frac{c}{H_o}\frac{1}{(1+z_{\rm rec})^{3/2}}\frac{1}{\Omega_{Mo}^{1/2}}\,, \tag{4}$$

d is of the order of 10^5 light years at recombination.

We can also compute the angular diameter distance of the last scattering surface:

$$D_A = \frac{c a_o r(z_{\rm rec})}{1+z_{\rm rec}}\,, \tag{5}$$

where

$$r(z) = [\sin(\chi)\ ;\ \ \chi\ ;\ \ \sinh(\chi)] \qquad [\Omega > 1\ ;\ \ \Omega = 1\ ;\ \ \Omega < 1] \tag{6}$$

and χ is the radial coordinate

$$\chi = \int_t^{t_o} \frac{{\rm d}t'}{a(t')} = \int_{a_o/(1+z)}^{a_o} \frac{{\rm d}a}{a^2(\dot a/a)}\,. \tag{7}$$

Once again, the Friedmann equation can be used to compute $\dot a/a$ and solve the integral for different values of the cosmological parameters:

$$\chi = \int_{a_o/(1+z)}^{a_o} \frac{{\rm d}\hat a}{H_o \hat a^2 \sqrt{\Omega_{\gamma o}\hat a^{-4} + \Omega_{Mo}\hat a^{-3} + \Omega_\Lambda + (1-\Omega)\hat a^{-2}}}\,. \tag{8}$$

These calculations confirm that the angle subtended by the acoustic horizon at recombination is of the order of one degree; moreover, for reasonable values of the other parameters, θ depends mainly on the density parameter Ω, and much less on the detailed budget of the different Ω_i. We thus expect features in the map of the CMB with a characteristic scale $\theta \sim 1^\circ$.

The power spectrum of the image of the CMB details the relative abundance of the spots with different angular scales. If we expand the temperature of the CMB in spherical harmonics,

$$\frac{\Delta T}{T} = \sum a_{\ell,m} Y_\ell^m(\theta,\phi)\,, \tag{9}$$

the power spectrum of the CMB is defined as $c_\ell = \langle a_{\ell,m}^2 \rangle$. The angular scale θ is related to the multipole ℓ as $\theta = \pi/\ell$. An angular scale of $\sim 1^\circ$ corresponds to a multipole $\ell \sim 200$. We thus expect a peak in the power spectrum of the CMB at a multipole ~ 200. Detailed models and codes are available to compute the angular power spectrum of the CMB image given a cosmological model for the generation of density fluctuations in the Universe, and a set of parameters describing the background cosmology [3].

The theory of acoustic oscillations in the primeval plasma predicts the presence of a *series* of peaks and dips in the power spectrum [7, 8]. This is because perturbations with different proper size enter the acoustic horizon (and start to oscillate) at different times before recombination, and have different oscillation periods. They thus arrive at recombination with a phase depending on their proper size. Perturbations with a size such that they arrive at recombination in a fully compressed phase or in a fully rarefied phase produce maximum deviations in the temperature of the CMB, thus producing maximum variance of the signal, *i.e.* peaks in the angular power spectrum.

This can be seen as a cosmic synchronization process, which starts the oscillation of small perturbations before the oscillation of large ones: the phase of the perturbations at the recombination depends on their intrinsic size. Perturbations with size close to the horizon at recombination start last, and have just enough time to arrive to the maximum

compression, producing the degree-size spots in the CMB, *i.e.* the first "acoustic" peak in the angular power spectrum of the CMB anisotropy. Perturbations with smaller intrinsic size have entered the acoustic horizon before, and arrive at recombination after a full compression and a return to the average density. They will produce a CMB temperature fluctuation smaller than the previous ones, because among the three physical processes producing temperature fluctuations from density ones, only the Doppler shift is effective. This corresponds to a dip in the angular power spectrum of the CMB at multipoles larger than the first acoustic peak. Even smaller perturbations have enough time to compress, return to the average density, and then arrive at the maximum rarefaction at recombination, producing a second peak in power spectrum, at multipoles about twice of those of the first one. Repeating this reasoning, we expect a harmonic series of acoustic peaks, up to very small sizes, smaller than the thickness of the last scattering surface. Photons diffusion, and the fact that many small-size positive and negative perturbations are aligned on the same line of sight, damps the temperature fluctuations measurable in the CMB at very high multipoles ($\ell \gtrsim 3000$).

The location of the first peak ℓ_1 shifts to lower multipoles (larger spots) as the density parameter increases. Physically, this is the result of Gravitational lensing of light rays coming from the LSS. The typical observed angular size of the hot and cold spots strongly depends on the average mass-energy density parameter Ω. The presence of mass and energy acts as a magnifying ($\Omega > 1$) or demagnifying ($\Omega < 1$) lens, producing horizon-sized spots larger or smaller than $\sim 1^\circ$ in the two cases, respectively.

It is interesting to see how the power spectrum depends on the other cosmological parameters.

Increasing the physical density of baryons $\Omega_b h^2$ favors compressions against rarefactions in the acoustic oscillations. Compression peaks are thus enhanced with respect to rarefaction ones. The relative amplitude of the second peak (rarefaction) with respect to the amplitude of the first peak (compression) is thus a good measurement of $\Omega_b h^2$. The power spectrum of primordial density fluctuations $P(k)$ controls the general shape of the power spectrum of the CMB.

The physical origin of density perturbations in the early Universe is unknown. An appealing hypothesis is that the Universe underwent an inflation phase immediately after the Big Bang. The Universe expanded so fast in this phase that all the Universe visible today was in a sphere of sub-atomic dimensions before the inflation phase. Quantum fluctuations in the inflaton field at microscopic scales before inflation are converted into adiabatic, scale invariant density fluctuations at cosmological scales after inflation. In this scenario the power spectrum of density fluctuations can be computed and is $P(k) = Ak^n$ with $n \sim 1$.

The value of n drives the amplitude of the higher order peaks in the power spectrum of the CMB relative to the amplitude of the first one. If only the first and second peak are observed, increasing n has about the same effect as decreasing $\Omega_b h^2$. A measurement of the third peak removes this degeneracy.

There is a strong degeneracy between cosmological parameters: different combinations of Ω_M, Ω_Λ, Ω and H_o can produce CMB power spectra almost identical, if the degeneracy factor R is the same (see [9]). For this reason, in addition to the CMB anisotropy and polarization measurements, which constrain mainly Ω, Ω_b and n, we will always need independent cosmological information, like the precision measurements of the Hubble constant (*e.g.*, from HST), the measurements of the deceleration parameter $q_o = -\ddot{a}a/\dot{a}^2|_{t_o} = \Omega_M/2 - \Omega_\Lambda$ (from high-z supernovae), the measurements of Ω_M (from cluster baryon fraction, cluster mass to light ratio, spectrum of density fluctuations,

peculiar velocities and bulk flows, etc.).

In this paper we describe observations of the CMB, which have recently measured the power spectrum, detected peaks in it, and constrained a number of cosmological parameters. We focus on the BOOMERanG experiment, which produced detailed maps of the microwave sky at 90, 150, 240 and 410 GHz, with angular resolution ~ 12 arcmin, and combined sensitivity $\sim 30\,\mu$K per pixel at 90 and 150 GHz. We describe the instrument and the observations, and we show that the 150 GHz map is dominated by fluctuations in the CMB. We describe the extraction of the angular power spectrum of the image of the CMB, and discuss its cosmological implications.

3. – CMB experiments

The detection of sub-horizon structures in the CMB is a difficult experimental problem. The size of the observable temperature fluctuations is of the order of a few tens μK, while instrumental, local and astrophysical backgrounds can be as large as few K. The differences in spectral and angular distributions allow the experimentalists to separate the cosmological component from the contaminations, but elaborate modulation techniques are needed [10-12]. Interferometers directly sample the correlation function of the temperature fluctuations [13], while total power receivers sample the temperature map: the power spectrum is derived by first organizing the time-ordered observations in a map and then performing the harmonic analysis.

The degree and sub-degree-scale anisotropy has now been detected by several ground-based and balloon-borne experiments. Only recently, however, it has been possible to first detect the presence of peaks in the power spectrum [14-16], and to produce images where the sub-degree anisotropy is clearly visible [17-24]. Full sky maps are expected from the NASA satellite MAP [25] early in 2003.

4. – BOOMERanG

The BOOMERanG experiment, a balloon-borne microwave telescope with cryogenic bolometric detectors, was flown on a long duration circum-Antarctic stratospheric balloon in 1998. The payload results from several experimental breakthroughs described in [26-28, 11, 29-31] (see fig. 1).

Modulation is achieved by scanning the sky at constant elevation and constant azimuth speed. The signal from the detector is AC coupled and high pass filtered. Since most of the contaminating signals are either constant or smooth in the sky, they are efficiently rejected by this modulation. The disadvantage of this technique is that it results in an anisotropic filtering of the sky maps, which has to be taken properly into account in the data analysis. It can be shown that, for our particular scan strategy, the time-domain high pass filter acts as a high pass filter in the multipoles domain [32].

A further level of modulation comes from sky rotation. In fact, the central azimuth of the azimuth scans tracks the azimuth of the best sky region, a high latitude region about $30^\circ \times 40^\circ$ wide and free from cirrus dust, centered at coordinates RA $\sim 85^\circ$, dec $\sim -45^\circ$. Elevation is not changed during the scan, and is only changed in steps every several hours. The result of this strategy is that, due to sky rotation, the scans are gradually tilted and offset in the sky, and the same pixel will be re-observed during the same day in differently tilted scans. This produces significant cross-linking in the sky coverage, which is important for the map-making algorithm used to create the image of the sky.

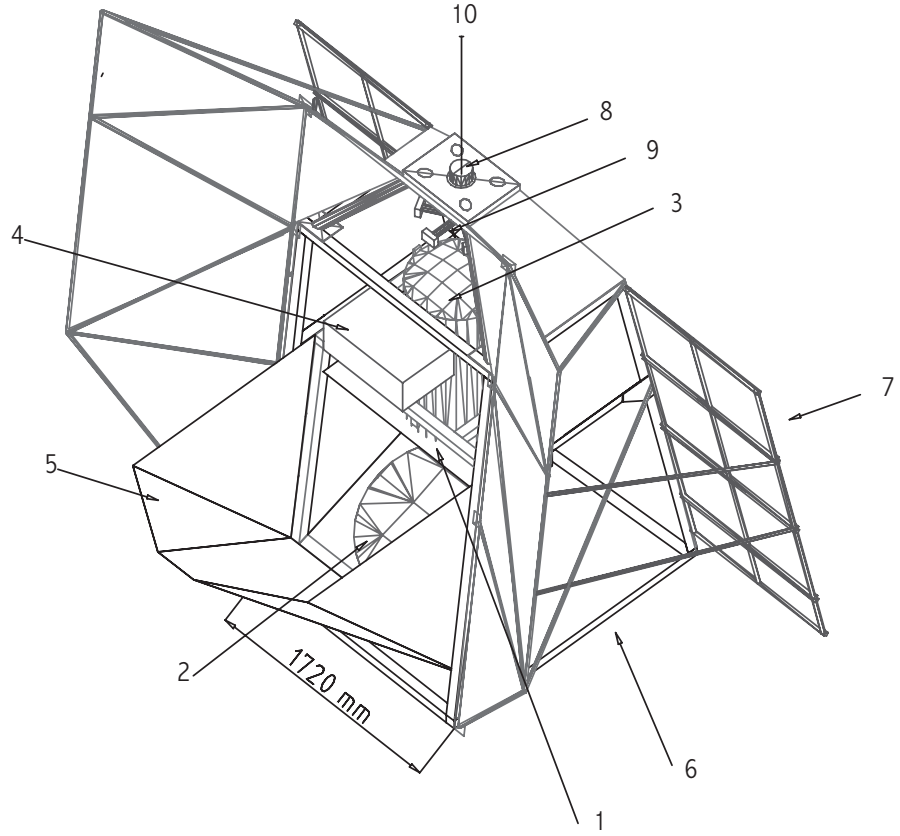

Fig. 1. – The BOOMERanG payload. On the inner frame (1) are mounted the off axis primary mirror (2), the cryostat with the detection system (3), the analog electronics (4), the ground shield (5). On the outer frame (6) are mounted the sun shields, the solar panels (7), the azimuth pivot (8) with the flywheel (9). The pivot decouples the payload from the flight chain (10).

The same process is repeated for several days. The comparison of maps obtained in different days, when the payload has drifted by thousands of km and the ground configuration is completely different, is a very effective tool to exclude contamination of the sky maps coming from signals in the telescope sidelobes.

The peak-to-peak length of our azimuth scans is $\Delta A \sim 60°$, so that the scans in the sky have a length $\Delta\theta \sim \Delta A \cos e \sim 42°$. This length has been selected as the best compromise between several factors: sky coverage, avoidance of the sun, repetition frequency of scans, detector's speed, $1/f$ knee in detectors noise, etc. As a result, our ℓ-space resolution is limited to $\Delta\ell \sim \pi/\Delta\theta \sim 4$. This is more than enough to resolve the acoustic peaks present in the power spectrum of the CMB anisotropy, which have a width $\Delta\ell_p \sim 100$ [33]. In practice, we degrade the instrumental resolution to $\sim \Delta\ell_p/2$ by binning in ℓ, in order to improve the signal to noise ratio in each ℓ bin. The estimates of the power spectrum averaged over wide ℓ bins are called bandpowers. The finite length of the scans also limits the lowest multipole detectable $\ell_{\min} \sim \Delta\ell$, but in practice a much higher $\ell_{\min} \sim 25$ is set by the presence of drifts and $1/f$ noise. The maximum multipole

observable in constant speed scans depends on the angular resolution of the telescope, on the time response of the detector [34] and on its noise; in general the sensitivity of the instrument to different multipoles is described by a suitable window function taking into account these effects (see below). In the case of BOOMERanG $\ell_{\rm max} \lesssim 1200$.

The BOOMERanG payload was flown by NASA-NSBF on Dec. 29, 1998, from McMurdo (Antarctica). It remained at float for 10.6 days, circumnavigating Antarctica at an average altitude of 37 km. About 57 million 16-bit samples of the signal were collected for each of the 16 detectors. The data were edited for known instrument glitches, temperature fluctuations, and cosmic rays events. Less than 5% of the bolometer data has been found to be contaminated. Constrained realizations of noise were substituted to the contaminated signals.

The pointing has been reconstructed from the signals of the laser gyroscopes, of the differential GPS, and of the sun sensors. In the most recent pointing solution, repeated observations of compact sources show that the accuracy of the reconstruction is $\lesssim 2.5$ arcmin *rms*. Random errors in the pointing have the effect to smear-out the signals from small sources. This adds in quadrature to the intrinsic angular resolution of the telescope ($9.5'$ FWHM at 150 GHz). The finite size of the pixelization has a similar effect. In ℓ space these three effects are modeled as a low pass filter, with a shallow cut-off at about $\ell \sim 600$. The time-domain high pass filter mentioned above acts as a sharper high-pass at multipole ~ 30. The result is a window function $W(\ell)$, which has to be taken into account in the reconstruction of the angular power spectrum of the sky. These effects limit the sensitivity of our observations at high multipoles. The result is that BOOMERanG is sensitive to a range of multipoles from $\ell = 50$ to $\ell = 1000$.

Sky maps have been constructed from the time ordered data and pointing using four independent methods: naive maps (just coadding data on the same pixel); maximum likelihood maps obtained using the MADCAP package [35]; maximum likelihood maps obtained using the iterative method of [36]; suboptimal maps obtained using the fast map making method of [32].

Degree-scale structures with amplitude of the order of $\sim 100\ \mu$K are evident in the map at 150 GHz (fig. 2). Consistent structure is also evident in the maps at 90 and 240 GHz. The similarity of the temperature maps obtained at different frequencies [17] is the best evidence for the CMB origin of the detected fluctuations. Foregrounds contamination can be constrained significantly in the center of the observed sky region [17], by comparison and correlation with dust templates [37]. Moreover, at variance with galactic maps, the fluctuations detected at 150 GHz pass several tests for Gaussianity [38]. We can even set upper limits to non Gaussian fluctuations mixed to the dominant Gaussian ones: the rms amplitude of the non-Gaussian component should be less than a few % of the rms amplitude of the Gaussian one.

The Gaussianity of the CMB temperature fluctuations is not trivial. As a matter of fact, if we do the Gaussianity analysis on sky brightness data with the same angular resolution, but in different regions of the em spectrum, we do find important deviations from Gaussianity. Our own 410 GHz channel is a good example of this behaviour [38]. The Gaussian character of the fluctuations is telling us something important about the cosmological origin of the fluctuations, and is in good agreement with the predictions of the simplest inflationary models.

Gaussianity also insures us that all the information encoded in the map is provided by the angular power spectrum of the map. We have computed the power spectrum of the sky by means of independent methods [35, 32], which rigorously take into account the effects of system noise, incomplete sky coverage, time-domain filtering of the data,

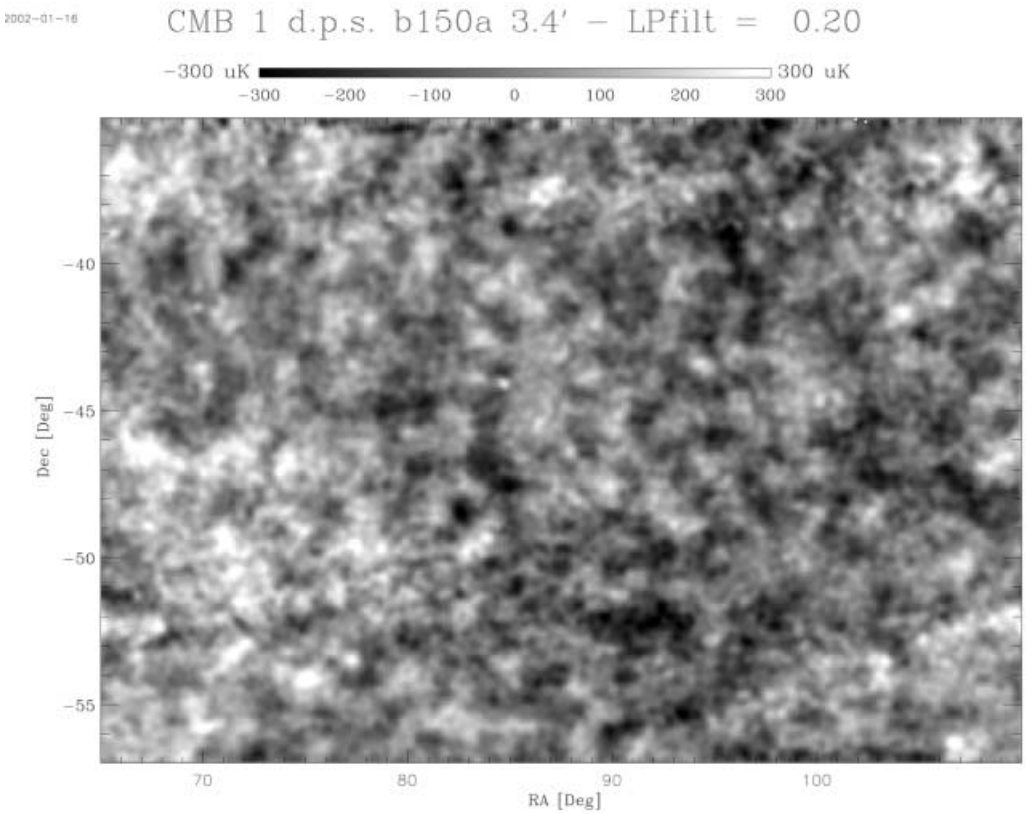

Fig. 2. – Map of the CMB at 150 GHz, as obtained from 4 channels of BOOMERanG.

beam shape etc. The current best spectrum of the sky is obtained from a combination of four channels at 150 GHz (fig. 3, see [19], for all the details of the analysis). In this spectrum, a peak at $\ell_{p1} \sim 213$ is evident at high statistical significance, and two further peaks at $\ell_{p2} \sim 541$, $\ell_{p3} \sim 845$ are also present at about 2σ significance [39]. They are interleaved with two dips at $\ell_{d1} \sim 416$ and $\ell_{d2} \sim 750$.

5. – Impact of the BOOMERanG results on cosmology

The simplest interpretation is that these features result from acoustic oscillations in the primeval plasma. The existence of these oscillations was predicted long time ago [7, 8, 40], and is expected in the standard inflationary scenario [41]. We derive the cosmological parameters within this theory framework, assuming adiabatic and Gaussian initial density fluctuations. With this assumption a full database of power spectra can be built by allowing each of the cosmological parameters to cover a wide range of values. The spectra are computed using the programs CMBFAST and CAMB [42, 43].

As explained in the introduction, the location of the first peak is directly related to the angular size of the acoustic horizon at recombination, and the comparison between linear and angular size of the horizon provides a clean way to measure Ω [5, 44]. In [17] we preliminarily derived Ω from the location of the first peak in the power spectrum derived

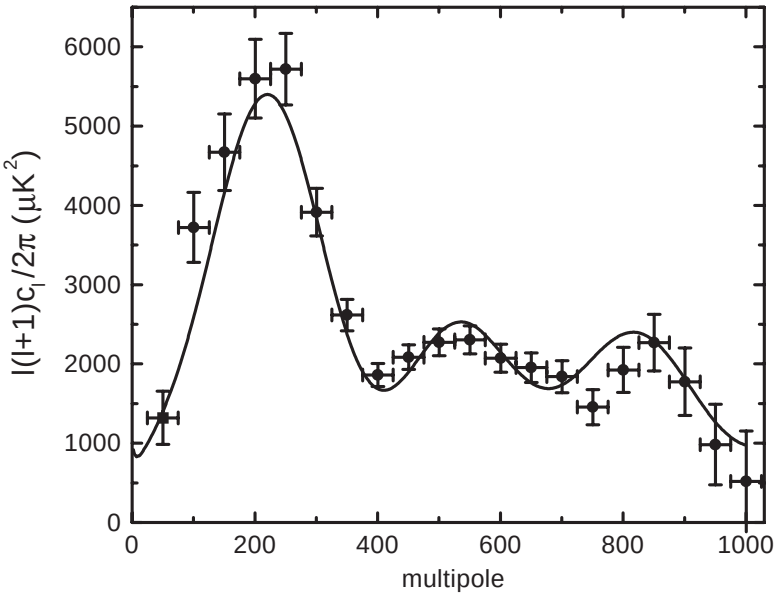

Fig. 3. – Angular power spectrum of the central part of the map of the CMB shown in fig.2. The continuous line is the best fit adiabatic inflationary model.

from the best data in the best 150 GHz channel. We also derived a set of cosmological parameters by means of a Bayesian analysis of the full power spectrum (for $\ell < 600$). While the results for Ω clearly indicated a flat geometry of the Universe, the results for other cosmological parameters (like $\Omega_b h^2$ and n_s) were still affected by calibration errors and degeneracy of the spectra due to limited multipoles coverage. In subsequent papers we derived the cosmological parameters from the full power spectrum of BOOMERanG (up to $\ell \sim 1000$). This was derived from the final BOOMERanG maps from 4 channels at 150 GHz, featuring improved beam and pointing reconstruction [19, 39]. The possibility to detect the third peak in the spectrum removed the degeneracy between $\Omega_b h^2$ and n_s. We find perfect consistency with a Euclidean universe: $\Omega = 1.02^{+0.05}_{-0.06}$. This result is very important for cosmology, since pre-CMB estimates of Ω ranged from 0.3 to 1.2. If we trust general relativity, the observation that $\Omega \sim 1$ today is very interesting. Our universe is following a very unstable solution of Einstein equations, and some mechanism (like inflation) has to be included in the standard Hot Big Bang scenario in order to explain this fact.

The second cosmological parameter well constrained by these data is the physical density of baryons: we find $\Omega_b h^2 = 0.022^{+0.004}_{-0.003}$. The density of baryons affects the symmetry of acoustic oscillations before recombination, thus controlling the ratio between the amplitudes of even and odd order peaks in the power spectrum. The density of baryons also controls the nuclear reactions happening in the first minutes after the Big Bang and producing the light elements. Measurements of the primordial abundance of elements allow to estimate $\Omega_b h^2$ with even higher precision. Recent observations of primordial deuterium from quasar absorption line systems suggest a value $\Omega_b h^2 = 0.020 \pm 0.002$ at the 95% C.L. [45]. It is remarkable that such orthogonal techniques produce very consistent results: in our view this is a strong indication of the overall

consistency of the hot big bang scenario.

The third parameter constrained is the spectral index of the power spectrum of primordial density perturbations. We find $n_s = 0.96 \pm 0.09$. In inflation models, the spectral index of the primordial fluctuations gives information about the shape of the primordial potential of the inflaton field which drove inflation. While there is no fundamental constraint on this parameter, the simplest models of inflation do give values that are just below unity.

Adding limited prior knowledge on the Hubble constant (*i.e.* $0.4 < h < 0.9$) and on the age of the Universe (*i.e.* $t > 10$ Gy) allows us to constrain significantly the density of dark matter and of dark energy. The result is a universe where ordinary matter accounts for only 4% of the total mass-energy density, while about 25% of the Universe is in the form of still undetected dark matter. A mysterious form of dark energy (*i.e.* something with negative pressure in the stress-energy tensor) accounts for the remaining $\sim 70\%$ of the mass-energy density.

6. – Experimental and cosmic consistency

The power spectrum results from BOOMERanG have now been confirmed and extended by independent experiments. The measurements of MAXIMA, DASI, VSA, CBI, Archeops [20, 46, 21-24] are all consistent with the power spectrum detected by BOOMERanG, when calibration errors are properly taken into account. Moreover, all these independent experiments find consistent estimates for the cosmological parameters. The apparently strange composition of the Universe is confirmed by independent cosmological observations (see, *e.g.*, [47-50]: the nature of dark matter and dark energy remain the most important open questions in cosmology and fundamental physics.

7. – The future

CMB experiments can improve our understanding of Nature in several ways. We will not even start to say how much the two CMB space mission (the ongoing MAP of NASA and the incoming Planck of ESA) will impact cosmology. They will provide full sky maps free of systematic effects, with high resolution, wide frequency coverage, and precise calibration, resulting in precision measurements of the CMB power spectrum and of the cosmological parameters.

The current data already hint to the nature of Dark Energy by constraining its equation of state (see, *e.g.*, [51]): increased precision will be possible with the high quality data MAP and Planck, and with the detection of a large number of high redshift supernovae with the SNAP satellite [52].

CMB Polarization measurements have just detected linear polarization at a level $\sim 10\%$ of the anisotropy [53]; further measurements, like the ones carried out by the new BOOMERanG payload (see, *e.g.*, [54, 55], will confirm the origin of the anisotropy and provide evidence for the type of perturbations (adiabatic vs isocurvature, for example) responsible for the initial density fluctuations. A window of opportunity for detection of inflation-generated gravity waves is open for higher precision polarization and anisotropy data [56, 51]. A subsequent generation of polarization experiments will provide deep insight on the physics of inflation (see, *e.g.*, [57]).

* * *

The BOOMERanG experiment is supported in Italy by Agenzia Spaziale Italiana, Programma Nazionale Ricerche in Antartide, Università di Roma "La Sapienza"; by PPARC in the UK, by NASA, NSF OPP and NERSC in the USA, and by CIAR and NSERC in Canada. The authors are deeply indebted with all the members of the BOOMERanG team (see [39] for the list of members) for years of intense and fruitful collaboration.

REFERENCES

[1] Tytler *et al.*, astro-ph/0001318 (2000).
[2] Mather J., astro-ph/9605054 (1996).
[3] Hu W. and Dodelson A., *Annu. Rev. Astron. Astrophys.*, astro-ph/0110414 (2002).
[4] E. W. Kolb and Turner M. S, *The Early Universe* (Addison-Wesley) 1990.
[5] Weinberg S., *Phys. Rev. D*, **62** (2000) 127302.
[6] Rich J., *Fundamentals of Cosmology* (Springer-Verlag, Berlin) 2001.
[7] Peebles P. J. E. and Yu J. T., *Astrophys. J.*, **162** (1970) 815.
[8] Doroshkevich A. G., Sunyaev R. A. and Zeldovich Ya. B., *Sov. Astron.*, **22** (1978) 523.
[9] Efstathiou G. and Bond J. R., *Mon. Not. R. Astron. Soc.*, **304** (1999) 75.
[10] Miller A. *et al.*, astro-ph/0108030 (2001).
[11] Piacentini F. *et al.*, *Astrophys. J. Suppl.*, **138** (2002) 315, astro-ph/0105148.
[12] Lee A. *et al.*, in *3K Cosmology*, *AIP Conf. Proc.*, Vol. **476** (1999); astro-ph/9903249.
[13] White M. *et al.*, astro-ph/9912422.
[14] Miller A. *et al.*, *Astrophys. J.*, **524** (1999) L1.
[15] Torbet E. *et al.*, *Astrophys. J.*, **521** (1999) L79.
[16] Mauskopf P. *et al.*, *Astrophys. J.*, **536** (2000) L59.
[17] de Bernardis P. *et al.*, *Nature*, **404** (2000) 955.
[18] Hanany S. *et al.*, *Astrophys. J.*, **545** (2000) L5.
[19] Netterfield B. *et al.*, *Astrophys. J.*, **571** (2002) 604.
[20] Leitch E. M. *et al.*, astro-ph/0104488 (2001).
[21] Scott P. F. *et al.*, submitted to *Mon. Not. R. Astron. Soc.*, astro-ph/0205380.
[22] Mason B. *et al.*, submitted to *Astrophys. J.*, astro-ph/0205384; Pearson T. J. *et al.*, submitted to *Astrophys. J.*, astro-ph/0205388.
[23] Benoit A. *et al.*, astro-ph/0210305 (2002).
[24] Benoit A. *et al.*, astro-ph/0210306 (2002).
[25] Page L., *Proc. IAU Symposium 201*, edited by A. Lasenby and A. Wilkinson, astro-ph/0012214 (2000).
[26] Mauskopf P. *et al.*, *Appl. Opt.*, **36** (1997) 765,
[27] Masi S. *et al.*, *Cryogenics*, **38** (1998) 319.
[28] Masi S. *et al.*, *Cryogenics*, **39** (1999) 217.
[29] Pascale E. and Boscaleri A., in *BC2K1*, *AIP Conf. Ser.*, edited by De Petris and Gervasi, *AIP Conf. Ser.*, Vol. **616** (2001), p. 56.
[30] Romeo G. *et al.*, in *BC2K1*, edited by De Petris and Gervasi, *AIP Conf. Ser.*, Vol. **616** (2001), p. 59.
[31] Crill B. *et al.*, astro-ph/0206254.
[32] Hivon E. *et al.*, astro-ph/0105302 (2001).
[33] Hu W., Sugiyama N. and Silk J., *Nature*, **386** (1997) 37.
[34] Hanany S., Jaffe A. and Scannapieco E., *Mon. Not. R. Astron. Soc.*, **299** (1998) 653, astro-ph/9801291.
[35] Borrill J., in *3K Cosmology*, astro-ph/9911389.
[36] Natoli P. *et al.*, submitted to *Astrophys. J.*, astro-ph/0101252 (2001).

[37] Masi S. *et al.*, *Astrophys. J.*, **553** (2001) L93, astro-ph/0101539.
[38] Polenta G. *et al.*, *Astrophys. J.*, **572** (2002) L27, astro-ph/0201133.
[39] de Bernardis P. *et al.*, *Astrophys. J.*, **564** (2002) 559.
[40] Silk J. and Wilson M. L., *Physica Scripta*, **21** (1980) 708.
[41] Bond J. R. and Efstathiou G., *Mon. Not. R. Astron. Soc.*, **226** (1987) 655.
[42] Seljak U. and Zaldarriaga M., *Astrophys. J.*, **469** (1996) 437.
[43] Lewis A., Challinor A. and Lasenby A., astro-ph/9911177.
[44] Melchiorri A. and Griffiths L. M., astro-ph/0011147 (2000).
[45] Burles S., Nollett K. M. and Turner M. S., astro-ph/0010171 (2000).
[46] Lee A. *et al.*, submitted to *Astrophys. J.*, astro-ph/0104459 (2002).
[47] Perlmutter S. *et al.*, *Astrophys. J.*, **483** (1997) 565.
[48] Perlmutter S. *et al.*, *Nature*, **391** (1998) 51.
[49] Garnavich P. M. *et al.*, *Astrophys. J. Lett.*, **493** (1998) L53.
[50] Riess A. G. *et al.*, *Astrophys. J.*, **116** (1998) 1009.
[51] Melchiorri A. *et al.*, astro-ph/0211522.
[52] http://snap.lbl.gov/satellite.html
[53] astro-ph/0209478, astro-ph/0209476.
[54] Masi S. *et al.*, in *Astrophysical Polarized Backgrounds, AIP Conf. Ser.*, Vol. **609**, edited by Cecchini, Cortiglioni, Sault and Sbarra (2001), pp. 122-127.
[55] Masi S. *et al.*, in *Experimental Cosmology at Millimetere Wavelengths, 2K1B2, AIP Conf. Ser.*, Vol. **616**, edited by De Petris and Gervasi (2001), pp. 168-174.
[56] Melchiorri A. and Odman C., astro-ph/0210606.
[57] Kamionkowski M. and Kosowski A., *Phys. Rev. D*, **67** (1998) 685.